Space-Time Block Coded Spatial Modulation for Indoor Visible Light Communications

Shimaa Naser, Lina Bariah, *Senior Member, IEEE*, Sami Muhaidat, *Senior Member, IEEE*, Mahmoud Al-Qutayri, *Senior Member, IEEE*, Murat Uysal, *Fellow, IEEE*, and Paschalis C. Sofotasios, *Senior Member, IEEE*

arXiv:2111.03928v1 [cs.IT] 6 Nov 2021

***Abstract*—Visible light communication (VLC) has been recognized as a promising technology for handling the continuously increasing quality of service and connectivity requirements in modern wireless communications, particularly in indoor scenarios. In this context, the present work considers the integration of two distinct modulation schemes, namely spatial modulation (SM) with space time block codes (STBCs), aiming at improving the overall VLC system reliability. Based on this and in order to further enhance the achievable transmission data rate, we integrate quasi-orthogonal STBC (QOSTBC) with SM, since relaxing the orthogonality condition of OSTBC ultimately provides a higher coding rate. Then, we generalize the developed results to any number of active light-emitting diodes (LEDs) and any M-ary pulse amplitude modulation size. Furthermore, we derive a tight and tractable upper bound for the corresponding bit error rate (BER) by considering a simple two-step decoding procedure to detect the indices of the transmitting LEDs and then decode the signal domain symbols. Notably, the obtained results demonstrate that QOSTBC with SM enhances the achievable BER compared to SM with repetition coding (RC-SM). Finally, we compare STBC-SM with both multiple active SM (MASM) and RC-SM in terms of the achievable BER and overall data rate, which further justifies the usefulness of the proposed scheme.**

***Index Terms*—MIMO, VLC, spatial modulation, repetition coding, SSK, STBCs.**

I. INTRODUCTION

Future sixth generation (6G) and beyond mobile communications are envisioned to witness a plethora of novel data-demanding applications that will be typically characterized by particularly stringent operational and quality of service requirements. This calls for the development of disruptive technologies that will be capable of catering for all anticipated demanding requirements, such as substantially higher data rates, ultra-low end-to-end latency, massive scale connectivity, increased robustness and expanded capacity, all under the umbrella of secure and energy efficient green communications [1], [2]. A key approach for meeting these requirements is through the radical shift from conventional radio frequency (RF) based communications, to more wideband communications using less occupied or unoccupied bands of the frequency spectrum.

Based on the above, recent advancements in solid state optical technology have facilitated the emergence of visible light communications (VLC), which is considered a promising breakthrough technology candidate for complementing RF wireless communications. In addition, relatively low deployment cost and ease of implementation can be realized in VLC systems by means of exploiting light emitting diodes (LEDs), which are primarily intended for illumination, in order to perform wireless transmission through intensity modulation and direct detection (IM/DD). Yet, despite the superior features of VLC, the performance of such systems is constrained by several factors, such as limited modulation bandwidth and restricted LED peak optical power, as well as by the imposed positive and real valued nature of transmitted signals [3]. Motivated by this, extensive research efforts have been devoted in order to enhance the performance of VLC systems by means of developing efficient optical-based modulation, coding, equalization, VLC cooperative communications, and multiple access (MA) schemes [4]–[6]. Additionally, the use of burst-mode receivers is particularly suitable for optical multi-access networks, which are based on packet transmission, as they are capable of enhancing the transmission data [7]. Finally, due to its high spectrum efficiency, simplified and efficient implementation, as well as inter-symbol interference mitigation capabilities, orthogonal frequency division multiplexing (OFDM) has been also investigated in the context of VLC. The work in [8] has considered the performance evaluation of different types of quadrature-amplitude modulation (QAM) and phase-shift keying (PSK) modulation with three different channel estimation methods in OFDM system aiming

This work was supported in part by Khalifa University under Grant KU/FSU-8474000122 and Grant KU/RC1-C2PS-T2/8474000137. *Corresponding Author: Paschalis C. Sofotasios.*

S. Naser and L. Bariah are with the Center for Cyber-Physical Systems, Department of Electrical Engineering and Computer Science, Khalifa University, Abu Dhabi 127788, UAE, (e-mails: 100049402@ku.ac.ae; lina.bariah@ieee.org.)

S. Muhaidat is with the Center for Cyber-Physical Systems, Department of Electrical Engineering and Computer Science, Khalifa University, Abu Dhabi 127788, UAE, and also with the Department of Systems and Computer Engineering, Carleton University, Ottawa, ON K1S 5B6, Canada, (e-mail: muhaidat@ieee.org).

M. Al-Qutayri is with the Systems-on-Chip (SoC) Center, Department of Electrical Engineering and Computer Science, Khalifa University, Abu Dhabi 127788, UAE, (e-mail: mahmoud.alqutayri@ku.ac.ae).

M. Uysal is with the Department of Electrical and Electronics Engineering, Ozyegin University, 34794 Istanbul, Turkey (e-mail: murat.uysal@ozyegin.edu.tr).

P. C. Sofotasios is with the Center for Cyber-Physical Systems, Department of Electrical Engineering and Computer Science, Khalifa University, Abu Dhabi 127788, UAE, and also with the Department of Electrical Engineering, Tampere University, Tampere 33014, Finland, (e-mail: p.sofotasios@ieee.org.)

to improve the overall throughput performance.

It is also recalled that multiple-input multiple output (MIMO) transmission techniques have been comprehensively studied in RF systems and they have been extensively shown to exhibit superior performance in terms of system capacity and reliability, compared to conventional single input single output (SISO) systems. Likewise, two MIMO strategies have been also proposed in the literature for VLC systems, namely, space time block codes (STBCs) and spatial multiplexing (SMP). On the one hand, SMP schemes are applied in VLC systems in order to accommodate the stringent demands for high data rate communications, by utilizing multiple LEDs in order to transmit different signals simultaneously. However, the simultaneous transmission from all LEDs results in a high inter-channel interference (ICI) and increased detection complexity [9]–[11]. On the other hand, STBCs schemes are privileged as they achieve an improved reliability, high data rate, ease of implementation, and reduced decoding complexity features [12], [13]. Existing results in the literature quantified the performance achieved enhancement by applying STBC over SISO systems in indoor VLC networks [14]–[16]. For instance, the work in [17] has jointly investigated STBCs with pulse position modulation (PPM). Results demonstrated the ability of the proposed scheme to achieve data rates of the order of hundreds of Mb/s in indoor VLC systems, while maintaining good link reliability. Furthermore, the authors in [18] proposed a quasi-trace-orthogonal-STBC, where the transmitted codewords follow the quasi-trace orthogonal property to provide an enhanced spectral efficiency. Corresponding simulations were experimentally tested for a 4×4 MIMO L-PPM VLC system. The proposed scheme showed an enhanced spectral efficiency performance of up to four times that of the trace-orthogonal STBC when 8-PPM was used.

Meanwhile, index modulation is considered an efficient modulation scheme for enhancing the spectral and energy efficiency of VLC systems while maintaining a reduced hardware complexity [19]–[21]. The key difference in index modulation schemes compared to conventional modulation schemes is that additional data can be conveyed over the indices of the major blocks of the communication system through on/off keying mechanism. These are, for example, the indices of the LEDs, frequency subcarriers, time slots, or a combination of them. Based on this, indexing in the spatial domain has been thoroughly investigated in the field of VLC networks [19]. Specifically, different forms of spatial index modulation have been proposed and investigated in the open literature, such as, space shift keying (SSK), generalized space shift keying (GSSK), and spatial modulation (SM) [22]. SSK is the simplest form of spatial domain index modulation where a single LED out of N_t LEDs is activated and the data is conveyed over the index of the activated LED. Yet, although SSK has the advantages of providing an interference free communication and simple receiver design, a large number of transmit LEDs is required to achieve higher modulation orders, and hence, high spectral efficiency. So, in the generalized case, i.e. in GSSK, N_a LEDs are activated simultaneously to boost the spectral efficiency at the expense of an incurred spatial interference [23]. In this context, various reported contributions investigated the performance capability of GSSK in VLC systems. For instance, [24] derived a closed form expression for the average symbol error rate (ASER) for direct-code GSSK system and showed that with a low complexity power allocation mechanism, the ASER and spectral efficiency can be improved significantly. Moreover, the authors in [25] investigated the physical layer security of a GSSK-VLC system and proposed an optimal LED pattern selection algorithm to enhance the achievable secrecy performance. A similar analysis was carried out in [26], wherein a novel spatial constellation design technique was proposed based on GSSK.

It is recalled that SM was firstly introduced by Mesleh $et\ al.$ in [27], as an efficient scheme to reduce the ICI introduced by SMP and overcome the spectral efficiency limitations of SSK and GSSK schemes. To achieve this, the principle of SM is based on conveying information in both the signal and spatial domains. A detailed comparison between SMP, repetition coding (RC) and SM was carried out in [4]. There, it was demonstrated that SM achieves compromised performance between spectral efficiency, error rate, and complexity. Likewise, the authors in [28] investigated the secrecy rate performance of SM and proposed channel adaptive selection and a greedy selection schemes for choosing the active transmitter in order to enhance the secrecy rate performance. In addition to this, it is also widely known that the performance of SM in VLC is highly affected by the incurred channel correlation. To overcome this issue, the authors in [29] proposed an alteration of the orientation of the photo-detector (PD), while an LED grouping based SM method was reported in [30]. Subsequently, the authors in [31] proposed an adaptive SM scheme that balances the trade-off between spectral efficiency and link robustness. In this scheme, the modulation size was dynamically changed based on the channel cumulative distribution function (CDF) of the user. Furthermore, additional studies on adaptive SM were also considered in [32] and [33]. Likewise, the integration of SM and non-orthogonal multiple access has been investigated in multi-user MIMO VLC networks as a means of enhancing the overall spectral efficiency of the system [34]–[36].

Following the same concept as in SSK, a single LED in SM is activated. However, the activated LED additionally sends a positive real-valued symbol, which ultimately results in an enhanced spectral efficiency compared to SSK modulation. In this context and in order to provide a more flexible system design, the authors in [37] proposed the activation of N_a LEDs out of the total N_t, while RC was applied in order to transmit the same M-ary symbol through the active LEDs. However, this scheme is still limited in terms of the achievable spectral efficiency since the same symbol is transmitted from all active LEDs. Furthermore, the error rate performance of RC-SM is practically degraded at higher spectral efficiency

values since higher M-ary modulation orders are required in order to maintain a certain high spectral efficiency under the same system setup.

Multiple active SM (MASM) is a more generalized version of conventional SM that highly enhances the spectral efficiency by conveying more information in both spatial and signal domains [5], [38], [39]. It is noted that MASM relies on the activation of N_a LEDs out of N_t, whilst multiple distinct real non-negative M-ary symbols are transmitted from each active LED. It was shown in [40], [41] that MASM achieves high spectral efficiency compared to other spatial index modulation schemes. However, its major drawback is the degraded bit error rate (BER) performance, particularly for a large number of activated LEDs and high modulation orders. The mentioned BER performance degradation results in a deterioration in the VLC system's throughput. In order to tackle this issue, a bit-to-symbol mapping based on the corresponding Euclidean distance (ED) was proposed for MASM in [42], where it was shown that the proposed MASM with ED-mapping outperforms conventional mapping for MASM. Additionally, the authors in [43] utilized multi-color LED (QLEDs) as transmitters in a MASM system. In their scheme, the optimal QLED pattern was selected according to the chromaticity property of the LEDs. However, this scheme exhibits increased complexity, so signal design schemes with reduced complexity are highly essential. Moreover, constellation design algorithms for single-mode and dual-mode joint MASM were proposed in [44] for the case of highly correlated VLC channels. On the contrary, an iterative combinatorial symbol design algorithm was proposed in [45]. In this context, the achievable symbol error rate (SER) performance was enhanced for a random symbol set by iteratively adding and removing symbols. Finally, the integration of MASM with orthogonal frequency division multiplexing scheme was considered in [46] and [47]. Based on this and according to the above discussion, there is an urgent need for the design of efficient modulation schemes in order to ultimately achieve an adequate balance between spectral efficiency enhancement, BER performance, and involved receiver complexity.

A. Contribution

As already mentioned, several MIMO transmission techniques have been proposed in the open literature to compensate for the spectral loss introduced by LEDs and the constraints imposed by intensity modulation direct detection (IM/DD). In addition, the MASM concept was recently proposed and was found capable of increasing the transmission data rate by means of conveying information in both signal and spatial domains. However, the main drawback of this scheme is the degraded error rate performance at higher spectral efficiency values. Based on this, the present contribution proposes space time block coded-spatial modulation (STBC-SM) for indoor VLC systems. It is worth mentioning here that the integration of STBC with SM is a particularly promising modulation scheme because it can achieve a significant performance enhancement over MASM by exploiting the advantages of both SM and STBC, while maintaining high energy efficiency and reduced complexity [48], [49]. However, an STBC-SM based scenario in the context of VLC has not been investigated in the literature so far. Therefore, the core aim of our work is to propose a comprehensive framework for the investigation of STBC-SM and for quantifying the advantages of integrating SM and STBC scheme in indoor VLC environments. In more details. the main contributions of this paper are summarized as follows:

- We propose an STBC-SM scheme for indoor VLC systems, which offers a trade-off between spectral efficiency, reliability, and receiver complexity.
- We generalize Alamouti STBC-SM to an arbitrary number of active LEDs. Moreover, we provide a general design for the M-ary pulse amplitude modulation (PAM) symbols and their complements.
- We propose the integration of quasi-orthogonal STBCs (QOSTBCs) with SM to further enhance the system spectral efficiency.
- We purpose a new receiver design based on two-step maximum likelihood (ML) decoding process to reduce the complexity associated with the conventional joint ML receivers.
- To corroborate the performance enhancement achieved by STBC-SM, we consider the proposed two-step ML detector to derive the pairwise error probability (PEP) of the active LEDs indices, which is then utilized to derive a union bound for the probability of incorrect index detection.
- Capitalizing on the derived union bound, we evaluate the probability of incorrect detection of the transmitted symbols, by deriving a tight and tractable bound for the corresponding BER.
- To compare their spectral efficiency performance, we provide an analysis for the achievable rate of MASM and STBC-SM schemes.
- Finally, we present extensive analytic and simulation results in order to validate the derived BER bound expression and to corroborate the BER superiority of the proposed scheme compared to the MASM counterpart as well as the achieved throughput enhancement at high M-ary PAM.

To the best of the authors' knowledge, the offered results have not been previously reported in the open technical literature. The remainder of this paper is organized as follows: Section II presents the considered system and channel models, whereas section III proposes the generalized STBCs and the QOSTBC for VLC systems. Section IV presents the proposed ML decoding along with the required steps for the derivation of the BER bound. Capitalizing on this, the corresponding analytic and simulation results are discussed in section V. Finally, the paper is concluded in section VI with some useful comments and suggestions.

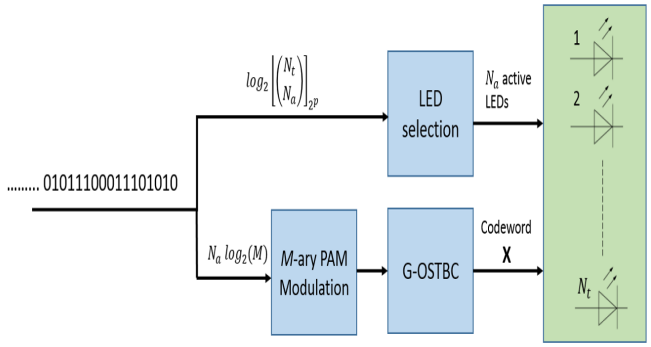


Fig. 1: Generalized STBC-SM transmitter

Notations: Throughout the manuscript, unless mentioned otherwise, boldface uppercase and lowercase represent matrices and vectors, respectively. Also, $(\cdot)^T$, $|\cdot|$, and $\|\cdot\|$ denote the transpose, the absolute value, and the norm operations, respectively whereas $\boldsymbol{I}$ denotes the identity matrix. The notations $\binom{N}{k}$ and $\lfloor x \rfloor_{2^p}$ represent respectively the binomial coefficient and the largest integer less than or equal x, that is integer power of 2. Finally, $\mathcal{N}(0, \sigma^2)$ denotes a real-valued Gaussian distribution with zero mean value and variance σ^2.

II. System and Channel Models

We consider an indoor VLC multiple-input single-output (MISO) downlink system which consists of N_t transmit LEDs, a single PD user ($N_r = 1$), and N_a active LEDs. Without loss of generality, the dimensions of the considered room in the present scenario are $5 \times 5 \times 4\ m^3$. The transmitted bit stream is divided into two parts; the first part consists of $\log_2(\lfloor \binom{N_t}{N_a} \rfloor_{2^p})$ bits, where $\lfloor \binom{N_t}{N_a} \rfloor_{2^p}$ denotes the number of combinations of N_t LEDs taken N_a at a time, which is less than or equal to $\binom{N_t}{N_a}$ and is power of 2. Those bits are used to select the LEDs' indices that will be activated. On the contrary, the other $(RN_a)\log_2(M)$ bits are modulated using M-ary PAM modulation and are then encoded using a STBC with coding rate of R. The generalized STBC-SM transmitter is depicted in Fig. 1. Therefore, the received signal can be written as follows

$$\mathbf{y} = \frac{\eta}{N_a} \mathbf{X}\ \mathbf{h}_\ell + \mathbf{z}, \tag{1}$$

where η is the PD responsivity and $\mathbf{X} \in \mathbb{R}^{T \times N_a}$ is the transmitted codeword, where T denotes the number of time slots. It is worth mentioning that the normalization by N_a is performed in order to guarantee fixed illumination in the room. Moreover, $\mathbf{z} \in \mathbb{R}^{T \times 1}$ represents the additive white Gaussian noise (AWGN) with zero mean and variance $\sigma^2 = \sigma^2_{shot} + \sigma^2_{th}$, where σ^2_{shot} and σ^2_{th} denote the variances of the shot noise and thermal noise, respectively. A detailed noise variance calculation was reported in [50]. Additionally, $\mathbf{h}_\ell \in \mathbb{R}^{N_a \times 1}$ denotes the channel gain vector between the N_a active LEDs and the PD, in which only the line of sight (LoS) component is considered. To this effect, each component of $\mathbf{h}_\ell$ can be expressed as [51]

$$h_i = \begin{cases} \frac{A}{d_i^2} R_o(\varphi_i) T_s(\phi_i) g(\phi_i) \cos(\phi_i), & 0 \leqslant \phi_i \leqslant \phi_c \\ 0, & \text{otherwise} \end{cases} \tag{2}$$

where A denotes the PD area, d_i is the distance between the ith active LED and the PD, φ_i is the angle of transmission from the ith active LED to the PD, ϕ_i is the incident angle with respect to the receiver, and ϕ_c is the field of view (FoV) of the PD. Moreover, $T_s(\phi_i)$ and $g(\phi_i)$ denote the gains of the optical filter and concentrator, respectively. The $g(\phi_i)$ term can be expressed as follows

$$g(\phi_i) = \begin{cases} \frac{n^2}{\sin^2(\phi_c)}, & 0 \leqslant \phi_i \leqslant \phi_c \\ 0, & \phi_i > \phi_c \end{cases} \tag{3}$$

where n represents the refractive index, and $R_o(\varphi_i)$ denotes the Lambertian radiant intensity. Further details about $R_o(\varphi_i)$ can be found in [50].

III. Generalized STBC for VLC Systems

It is recalled that STBCs have attracted considerable attention because of their demonstrated implementation and decoding simplicity, which renders them particularly capable of exploiting the distinct potentials of MIMO systems. In this context, orthogonal STBCs (OSTBCs) constitute special cases of STBCs which allow single-symbol simplified linear decoding. However, it is noted that OSTBCs in VLC systems can achieve a maximum coding rate of one. Therefore, high coding rate STBCs are required in order to provide higher transmission data rates. Thus, in this section we first generalize Alamouti STBC to an arbitrary M-ary PAM size. Subsequently, we consider the general case of an arbitrary number of active LEDs in order to develop the codeword for any optical OSTBCs. Finally, we propose a rate-2 QOSTBC that will enable an enhancement on the achievable transmission data rate.

To that end, starting with the well-known Alamouti STBC, the transmitted codeword from two active LEDs can be expressed as

$$\mathbf{X}_2 = \begin{bmatrix} x_1 & x_2 \\ \bar{x_2} & x_1 \end{bmatrix}, \tag{4}$$

where x_1 and x_2 are real and positive PAM symbols. Moreover, $\bar{x_i}$ denotes the complement of x_i, which for the special case of on-off keying (OOK) is calculated as $\bar{x_i} = I_p - x_i$, where I_p is the mean optical power. Also, x_i and $\bar{x}_i$ can be generalized into any PAM size M, so the intensity levels for the case of M-ary PAM are defined as follows

$$x_i \in \frac{2iI_p}{M-1},\ i = 0, 1, ..., (M-1). \tag{5}$$

It is noted here that when the LEDs transmit bits corresponding to the first level (i.e. $x_i = 0$), they will be incorrectly decoded as inactive. Therefore, in order to overcome this issue

and allow the receiver to distinguish the active LEDs, the intensity levels are modified as follows

$$x_i \in \frac{2iI_p}{M+1},\ i = 1, 2, ..., M \tag{6}$$

and the complement of the symbol x_i is

$$\begin{aligned} \bar{x_i} &= -x_i + \frac{2I_p}{M+1} + \frac{2MI_p}{M+1} \\ &= -x_i + 2I_p,\ \ i = 1, 2, ..., M. \end{aligned} \tag{7}$$

A. Optical Orthogonal STBCs

Alamouti STBC can be generalized to produce an $N_a \times N_a$ OSTBC of rate $R = 1$, which can be expressed as

$$\mathbf{X_{N_a}} = \begin{bmatrix} \mathbf{X}^1_{\frac{N_a}{2}} & \mathbf{X}^2_{\frac{N_a}{2}} \\ (\bar{\mathbf{X}}^2_{\frac{N_a}{2}})^T & (\mathbf{X}^1_{\frac{N_a}{2}})^{\hat{T}} \mathbf{X_{N_a}} \end{bmatrix} \in \mathbb{R}^{N_a \times N_a}, \tag{8}$$

where $\mathbf{X}^1_{\frac{N_a}{2}}$ and $\mathbf{X}^2_{\frac{N_a}{2}}$ are the $(N_a/2 \times N_a/2)$ OSTBC matrices for the first $N_a/2$ and the last $N_a/2$ symbols, respectively. The process starts by dividing the $N_a \times N_a$ matrix into blocks of size $N_a/2 \times N_a/2$. Then, each block is also divided into new sub-blocks until the smallest sub-block, i.e the Alamouti codeword is reached. In the present analysis, and without loss of generality, we consider the special case of an 8×8 OSTBC matrix. To this end, we fist start by dividing the 8×8 OSTBC matrix into blocks of size 4×4 as follows:

$$\mathbf{X_8} = \begin{bmatrix} \mathbf{X}^1_4 & \mathbf{X}^2_4 \\ (\bar{\mathbf{X}}^2_4)^T & (\mathbf{X}^1_4)^T \end{bmatrix}, \tag{9}$$

where $\mathbf{X}^1_4$ and $\mathbf{X}^2_4$ are 4×4 codewords for (x_1, x_2, x_3, x_4) and (x_5, x_6, x_7, x_8), respectively. Then, each block is divided into a smaller 2×2 OSTBC sub-blocks, which yields

$$\mathbf{X^1_4} = \begin{bmatrix} \mathbf{X}^1_2 & \mathbf{X}^2_2 \\ (\bar{\mathbf{X}}^2_2)^T & (\mathbf{X}^1_2)^T \end{bmatrix}, \mathbf{X^2_4} = \begin{bmatrix} \mathbf{X}^3_2 & \mathbf{X}^4_2 \\ (\bar{\mathbf{X}}^4_2)^T & (\mathbf{X}^3_2)^T \end{bmatrix}, \tag{10}$$

where $\mathbf{X}^1_2$ and $\mathbf{X}^2_2$ are Alamouti codewords for (x_1, x_2) and (x_3, x_4), respectively. On the contrary, $\mathbf{X}^3_2$ and $\mathbf{X}^4_2$ are Alamouti codewords for (x_5, x_6) and (x_7, x_8), respectively. Meanwhile, OSTBC codes for real symbols of rate $R = 1$ for N_a =3, 5, 6, and 7 can be obtained by eliminating some of the columns of the square OSTBC matrices defined earlier for $N_a = 4$ and 8 in (10) and (9), respectively. For example, a 4×3 OSTBC can be generated by eliminating the last column of the 4×4 OSTBC, yielding

$$\mathbf{X_3} = \begin{bmatrix} x_1 & x_2 & x_3 \\ \bar{x_2} & x_1 & \bar{x_4} \\ \bar{x_3} & x_4 & x_1 \\ \bar{x_4} & \bar{x_3} & x_2 \end{bmatrix}. \tag{11}$$

Importantly, the generated codewords satisfy the orthogonality condition $\mathbf{X_i^T X_i} = \mathbf{I}$. Therefore, they can be exploited for integrating STBC with SM in order to simplify receiver design and to allow the transmission of higher order modulation, as presented in detail in the following section.

B. Optical Quasi-Orthogonal STBCs

Despite their simplified ML detection, OSTBCs in VLC can achieve maximum coding rate of 1. Therefore, in order to provide higher rates the orthogonality is relaxed in order to transmit more symbols in each time slot through developing QOSTBCs. It is worth mentioning that QOSTBCs allow a trade-off between higher rates and decoding complexity; this is because parallel ML detectors are needed to jointly decode pairs (or more) of the transmitted symbols instead of single-symbol decoding as in OSTBCs. In what follows, we provide an example of a QOSTBC that achieves a rate $R = 2$, which is then utilized to be integrated with SM.

1) Rate-2 QOSTBC: A rate-2 QOSTBC for real symbols and two transmit LEDs is expressed as

$$\mathbf{X} = \begin{bmatrix} ax_1 + bx_3 & ax_2 + bx_4 \\ c\bar{x}_2 + d\bar{x}_4 & cx_1 + dx_3 \end{bmatrix}. \tag{12}$$

Of note, equation (12) is simply a linear combination of two optical Alamouti STBCs. Moreover, the parameters a, b, c, and d need to be carefully chosen in order to maximize the coding gain, while they also satisfy a fixed average transmitted optical power, i.e., $a + b = c + d = 1$. In order to simplify the detection process, we can choose $a = c$ and $b = d$. Therefore, the multiplication of the effective channel gain matrix and its transpose can be expressed as in (13), at the top of the next page. It is also worth noting that the values of the design parameters a, b, c, and d need to be optimized in order to obtain best detection performance. Also, it can be noticed from (13) that the joint ML decoding of the symbols x_1 and x_3 will be independent of the other two symbols, x_2 and x_4.

IV. Proposed ML Decoding for STBC-SM Scheme

In this section, we investigate the integration of STBC with SM in order to enhance the achievable VLC system performance in terms of reliability, throughput and complexity. To this end and by assuming that ML detection is utilized at the receiver side, the detector performs joint detection to deduce the received signals over the space and signal domains. In particular, the receiver will jointly detect the LED index and the transmitted symbol according to the following criterion

$$[\hat{\ell}, \hat{\mathbf{X}}] = \arg \min_{\tilde{\ell} \in \ell, \tilde{X} \in \mathbb{X}} \left\| \mathbf{y} - \frac{\eta}{N_a} \tilde{\mathbf{X}} \mathbf{h}_{\tilde{\ell}} \right\|^2, \tag{14}$$

where ℓ denotes the index of the transmitting LEDs and $\mathbf{X}$ is the transmitted codeword. It also recalled here that joint ML detection requires the search over all $M^{(R \times N_a)} \times \lfloor \binom{N_t}{N_a} \rfloor_{2^p}$ combinations, which results in a significantly increased receiver complexity. Yet, the orthogonal property of the generated OSTBC codewords and being of rate $R = 1$ allows the symbols x_i's to be decoded independently. This ultimately reduces the complexity to $M \times N_a \times \lfloor \binom{N_t}{N_a} \rfloor_{2^p}$. To this effect

$$\mathbf{H}_{eff}^{T}\mathbf{H}_{eff}=\begin{bmatrix}(ah_1)^2+(ch_2)^2 & 0 & abh_1^2+cdh_2^2 & 0\\ 0 & (ch_1)^2+(ah_2)^2 & 0 & cdh_1^2+abh_2^2\\ abh_1^2+cdh_2^2 & 0 & (bh_1)^2+(dh_2)^2 & 0\\ 0 & cdh_1^2+abh_2^2 & 0 & (dh_1)^2+(bh_2)^2\end{bmatrix}. \tag{13}$$

and aiming at reducing receiver complexity, we propose a detection mechanism in which the detection process is broken down into two main stages. The first stage comprises a conditional ML detection, in which conditioned on $\mathbf{X}$, the receiver detects only the indices of the transmitting LEDs as follows:

$$\hat{\ell}=\arg\min_{\tilde{\ell}\in\ell}\left\|\min_{X\in\mathbb{X}}[(\mathbf{y}-\frac{\eta}{N_a}\mathbf{X}\mathbf{h}_{\tilde{\ell}})|\mathbf{X}]\right\|^2. \tag{15}$$

In the second stage, the orthogonality of the generated STBC codewords is utilized to decouple the transmitted symbols. Based on this and by assuming perfect detection of the LEDs indices, and therefore perfect estimation of the channel matrix, the transmitted codeword can be evaluated as follows:

$$\mathbf{H}_{\ell_{\mathbf{eff}}}^{\mathbf{T}}\mathbf{y}=\check{\mathbf{y}}=\|\mathbf{h}_\ell\|^2\ \frac{\eta}{N_a}\ \mathbf{I}\,\mathbf{x}+\mathbf{z}, \tag{16}$$

where, $\mathbf{x}$ is the transmitted symbols vector, $\mathbf{x}=[x_1,x_2,...x_{\mathrm{N_a}}]^T$ and $\mathbf{z}\in\mathbb{R}^{T\times 1}$ is the AWGN vector, in which each component has a zero mean and a variance of $\sigma^2.\|\mathbf{h}_\ell\|^2$. Also, $\mathbf{H}_{\ell_{\mathbf{eff}}}\in\mathbb{R}^{T\times N_{ov}}$ is the effective channel gain matrix for the OSTBC, where N_{ov} denotes the overall number of symbols transmitted in T time slots. Finally, in order to detect the transmitted symbols, a conventional signal domain ML detector is utilized to decide on each transmitted symbol separately, namely

$$\hat{x_i}=\arg\min_{\tilde{x_i}\in\chi}\left|\check{y_i}-\|\mathbf{h}_\ell\|^2\ \frac{\eta}{N_a}\tilde{x_i}\right|^2. \tag{17}$$

It is also emphasized here that the proposed detector reduces the receiver complexity to $M\times Na+\lfloor\binom{N_t}{N_a}\rfloor_{2^p}$. Furthermore, if the QOSTBC defined in (12) is integrated with SM, the complexity is reduced to $2\times(M\times Na)+\lfloor\binom{N_t}{N_a}\rfloor_{2^p}$.

In what follows, we evaluate the BER performance of the proposed receiver for STBC-SM-based indoor VLC system.

A. BER Analysis

The probability of incorrect detection of the transmitted symbols can be evaluated as

$$P_e=P_{\mathbf{X}}(\mathbf{X}|\ell\neq\hat{\ell})P_\ell+P_{\mathbf{X}}(\mathbf{X}|\ell=\hat{\ell})(1-P_\ell), \tag{18}$$

where P_ℓ is the probability of incorrect index detection and $P_{\mathbf{X}}(\mathbf{X}|\ell=\hat{\ell})$ and $P_{\mathbf{X}}(\mathbf{X}|\ell\neq\hat{\ell})$ denote the probability of incorrect codeword detection conditioned on correct and incorrect index detection, respectively. Due to mathematical intractability of (18) and given that $P_{\mathbf{X}}(\mathbf{X}|\ell\neq\hat{\ell})$ is rather large, i.e. close to unity, the total error probability can be simplified as

$$P_e\leqslant P_\ell+P_{\mathbf{X}}(\mathbf{X}|\ell=\hat{\ell})(1-P_\ell). \tag{19}$$

Therefore, obtaining the BER from (19) requires the derivation of two expressions for P_ℓ and $P_{\mathbf{X}}(\mathbf{X}|\ell=\hat{\ell})$. To this effect and given that P_ℓ is conditioned on $\mathbf{X}$, we resort to the corresponding PEP, which represents an accurate metric to quantify the BER performance of a wireless system [52]. In fact, the derivation of the PEP constitutes the fundamental step for the derivation of a union bound on the BER.

Proposition 1. *The following closed-form expression is valid for the union bound of the BER for P_ℓ:*

$$P_\ell=\frac{1}{N2^N}\sum_{\forall\ell}\sum_{\ell\neq\hat{\ell}}D(\ell,\hat{\ell})Q\left(\sqrt{\frac{\eta^2}{4N_a^2\sigma^2}\left\|\mathbf{X}\mathbf{h}_\ell-\hat{\mathbf{X}}_{min}\mathbf{h}_{\hat{\ell}}\right\|^2}\right) \tag{20}$$

where $D(\ell,\hat{\ell})$ is the number of different bits between two distinct symbols.

Proof. With the aid of PEP, the upper bound to the probability of a union of all events of decoding ℓ as $\hat{\ell}$ can be represented as

$$P_\ell=\frac{1}{N2^N}\sum_{\forall\ell}\sum_{\ell\neq\hat{\ell}}D(\ell,\hat{\ell})P(\ell\longrightarrow\hat{\ell}), \tag{21}$$

where $P(\ell\longrightarrow\hat{\ell})$ is the PEP for index detection, which can be written as

$$P(\ell\longrightarrow\hat{\ell})=P\left(\left\|\mathbf{y}-\frac{\eta}{N_a}\hat{\mathbf{X}}_{min}\mathbf{h}_{\hat{\ell}}\right\|^2\leqslant\left\|\mathbf{y}-\frac{\eta}{N_a}\mathbf{X}_{min}\mathbf{h}_\ell\right\|^2\right). \tag{22}$$

After substituting the received signal $\mathbf{y}$ from (15) in (22), the PEP can be written as

$$P(\ell\longrightarrow\hat{\ell})=P\left(\left\|\frac{\eta}{N_a}\mathbf{X}\mathbf{h}_\ell+\mathbf{n}-\frac{\eta}{N_a}\hat{\mathbf{X}}_{min}\mathbf{h}_{\hat{\ell}}\right\|^2\leqslant\|\mathbf{n}\|^2\right). \tag{23}$$

Based on this and after some algebraic manipulations, the PEP can be expressed in closed form in terms of the one dimensional Gaussian $Q-$function, namely

$$P(\ell\longrightarrow\hat{\ell})=Q\left(\sqrt{\frac{\eta^2}{4N_a^2\sigma^2}\left\|\mathbf{X}\mathbf{h}_\ell-\hat{\mathbf{X}}_{min}\mathbf{h}_{\hat{\ell}}\right\|^2}\right). \tag{24}$$

Finally, the obtained PEP in (24) can be substituted in (21),

which yields the closed form representation in (20), which completes the proof. □

By leveraging the orthogonality feature of the STBC codewords defined in III.A, transmitted symbols can be decoded separately using the ML detector in (17). Therefore, the BER expression of M-ary PAM can be utilized in evaluating the probability of incorrectly detecting $\mathbf{X}$, namely [50]

$$P_{\mathbf{X}}(\mathbf{X}|\ell=\hat{\ell}) = \frac{2(M-1)}{M\log_2(M)} Q\left(\sqrt{\frac{\eta^2 \left\|\mathbf{h}_l\right\|^2 I_p^2}{N_a^2(M+1)^2\sigma^2}}\right). \quad (25)$$

Therefore, with the aid of (19), (20) and (25), the overall BER upper bound is given by the explicit expression in (26), at the top of the next page.

B. Achievable Rate Analysis for MASM and STBC-SM

Motivated by the advantages of MASM in improving the system's spectral efficiency, in this section we derive the rate expression for MASM and STBC-SM schemes and compare them in terms of their achievable spectral efficiency. To this end, it is recalled that the spectral efficiency for MASM depends on the activation patterns and the modulation size, namely

$$\eta_{masm} = N_a \log_2(M) + \log_2 \left\lfloor \binom{N_t}{N_a} \right\rfloor_{2^p}. \quad (27)$$

Based on this and given that the rate of correctly detected bits experiences severe degradation for the case of a large number of active LEDs and modulation size, the achievable rate of MASM can be evaluated in terms of the error probability as

$$R_{masm} = (1 - P_e^{masm}) \times \eta_{masm}, \quad (28)$$

where P_e^{masm} is the BER for a MASM system, which is expected to be particularly high for large M values. Following the same steps, the achievable rate of STBC-SM is given by

$$R_{stbc-sm} = (1 - P_e) \times \eta_{stbc-sm}, \quad (29)$$

where $\eta_{stbc-sm}$ is the spectral efficiency of STBC-SM, which can be expressed as

$$\eta_{stbc-sm} = \frac{R \times N_a \log_2(M) + \log_2(\lfloor \binom{N_t}{N_a} \rfloor_{2^p})}{T} \quad (30)$$

Therefore, it is noted that since STBC-SM scheme achieves a better BER performance for high M values compared to MASM and RC-SM, STBC-SM outperforms both schemes in terms of the corresponding BER, and hence the overall achievable rate. In addition, since the proposed QOSTBC in (12) has a rate of 2, when integrated with SM it will require lower modulation size compared to RC-SM to achieve the same spectral efficiency. This will be reflected on the error rate performance at high spectral efficiency values, as it is demonstrated in the next section.

It is noted here that evaluating the error rate performance with respect to the average electrical received signal-to-noise ratio (SNR) would disregard the individual path loss of the different setups and activated LEDs pattern. Therefore, in order to guarantee fair comparison, we opt to evaluate the error rate performance of the proposed scheme with respect to the transmit SNR, which is defined as the ratio of the average symbol energy against the noise power spectral density [4], [53]. It is also noted that the value of the transmit SNR in VLC systems is considerably higher than the one encountered in typical RF communication systems as it often exceeds 100 dB [54]. This is attributed to the small value associated with the noise power spectral density N_0 [55]. Specifically, by neglecting the photodetector dark current, N_0 is expressed as $N_0 \simeq q\ I_B$, where $q = 1.6e{-}19$ is the charge of electron and I_B is the background noise current that takes typical values in the order of μA [50], [56].

V. Numerical Results

In this section, we capitalize on the offered results to analyze the achievable performance of the proposed STBC-SM scheme. Hence, the validity of the derived analytic expressions in (26), (28) and (29) is first justified through extensive comparisons with respective results from computer simulations. To that end and without loss of generality, we consider an indoor VLC environment with dimensions of $5 \times 5 \times 4\ m^3$, in which the locations of both the involved LEDs and the user are illustrated in Fig. 2. In addition, it is assumed that the transmit LEDs radiate downward from the ceiling to the floor. On the contrary, the receiver position in the room is considered to be fixed throughout simulations and is assumed to be located at height of 0.8 m from the floor. Based on this, the corresponding channel gain can be also considered fixed. The receiver is also assumed to be oriented upward to the ceiling. Moreover, the LEDs semi-angle at half power $\varphi_{1/2}$ and the FoV of the PD are set to 60^o, which is a typical value for commercially-available high-brightness LEDs. For convenience, all the parameters involved in our simulations are summarized in Table I.

TABLE I: Simulation parameters.

Parameter	Symbol	Value
Room dimensions	-	$5 \times 5 \times 4m^3$
LED beam angle	$\varphi_{1/2}$	60^o
PD area	A	$1\ cm^2$
Refractive index of PD	n	1.5
Gain of optical filter	$T_s(\phi_i)$	1
FoV of PD	ϕ_c	60^o
PD responsitivity	η	$1A/W$

Fig. 3 shows the achievable analytic and simulated BER versus the transmit SNR for different modulation size with $N_T = 6, N_a = 2$ and $N_r = 1$. It is noticed that the derived formula in (26) forms an upper bound for the BER, which is tight at high SNR values for various modulation size. Additionally, STBC-SM enjoys a good performance in the range of interest of the transmit SNR for VLC system.

Next, a comparison between MASM and STBC-SM systems is considered in terms of the BER performance. The results are demonstrated in Fig. 4, where it is shown that

$$P_e \leqslant \frac{1}{N2^N}\sum_{\forall \ell}\sum_{\ell \neq \hat{\ell}} D(\ell,\hat{\ell}) Q\left(\sqrt{\frac{\eta^2}{4N_a^2\sigma^2}\left\|\mathbf{X}\mathbf{h}_\ell - \hat{\mathbf{X}}_{min}\mathbf{h}_{\hat{\ell}}\right\|^2}\right) + \frac{2(M-1)}{M\log_2(M)} Q\left(\sqrt{\frac{\eta^2\left\|\mathbf{h}_l\right\|^2 I_p^2}{N_a^2(M+1)^2\sigma^2}}\right) \times \left[1 - \frac{1}{N2^N}\sum_{\forall \ell}\sum_{\ell \neq \hat{\ell}} D(\ell,\hat{\ell}) Q\left(\sqrt{\frac{\eta^2}{4N_a^2\sigma^2}\left\|\mathbf{X}\mathbf{h}_\ell - \hat{\mathbf{X}}_{min}\mathbf{h}_{\hat{\ell}}\right\|^2}\right)\right]. \tag{26}$$

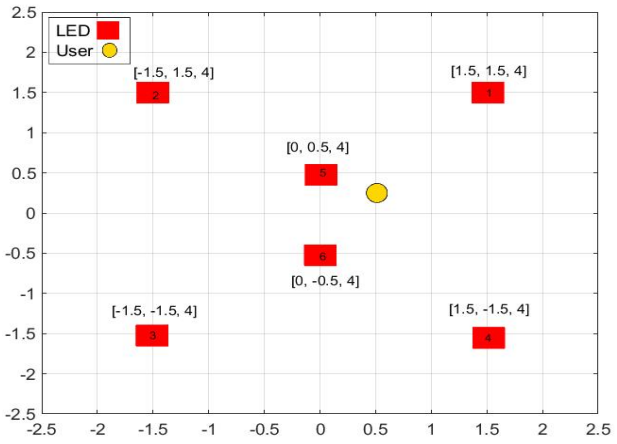


Fig. 2: LEDs and user placements in $5 \times 5 \times 4\ m^3$ room.

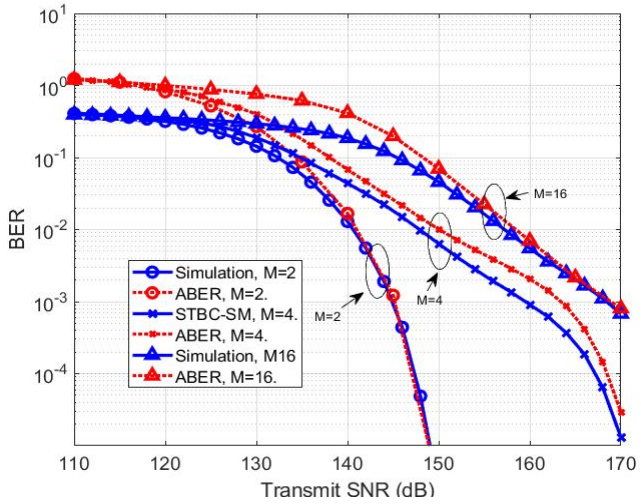


Fig. 3: Comparison between the derived analytical results and simulations. $N_T = 6$, $N_a = 2$, and $N_r = 1$.

integrating STBC with SM provides a significant BER improvement for large modulation size M. On the contrary, the illustrated performance of the corresponding MASM counterpart exhibits a deteriorated performance at high M values. For instance, for the case of $M = 2$, more than 20 dB is required to achieve a BER of 10^{-3} using MASM compared to STBC-SM. Additionally, STBC-SM user exhibits a good BER performance in the typical transmit SNR range for VLC system, where the received SNR in this case has an offset of 120 dB, since the channel gain is in the order of 10^{-6}.

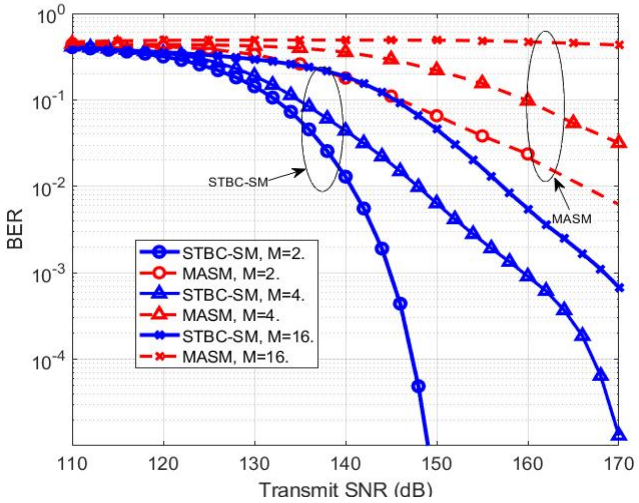


Fig. 4: BER performance comparison versus transmit SNR. $N_t = 6$, $N_a = 2$, and $N_r = 1$.

For fair comparison, we also consider the BER performance for both schemes for a fixed spectral efficiency η of 4 bpcu and 5 bpcu, as depicted in Fig. 5. We observe that, STBC-SM provides a reliability enhancement of the considered VLC systems compared to MASM, in the typical SNR range. For instance, for η = 4 bpcu at transmit SNR = 160 dB, the BER performance for STBC-SM and MASM is 10^{-4} and 10^{-3}, respectively i.e. a difference of around one order of magnitude. Moreover, a comparison in terms of the achievable throughput, as defined in (28) and (29), for both schemes is illustrated in Fig. 6. It is noted that in the typical SNR range, the throughput gap between the two schemes decreases as the modulation size increases, which is due to the high BER that occurs in the case of MASM. Meanwhile, using STBC with SM improves the BER performance, which is reflected on the achievable data rate as seen from (29).

In order to study the effect of various system parameters, namely N_t, N_a, and M, on the overall system performance we summarize the BER and the throughput performances for both STBC-SM and MASM schemes in Table II. It can be noticed that the proposed scheme provides a significant enhancement on the BER performance compared to MASM for different values of the involved parameters. For instance,

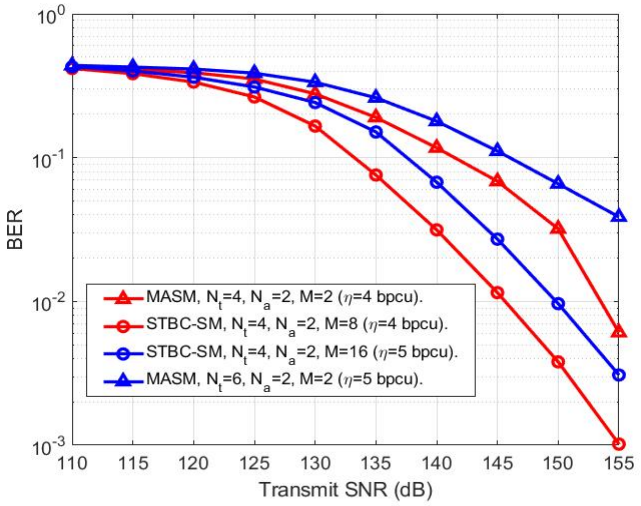


Fig. 5: BER performance comparison between STBC-SM and MASM for spectral efficiencies of 4 bpcu and 5 bpcu. Red lines for 4 bpcu, blue lines for 5 bpcu.

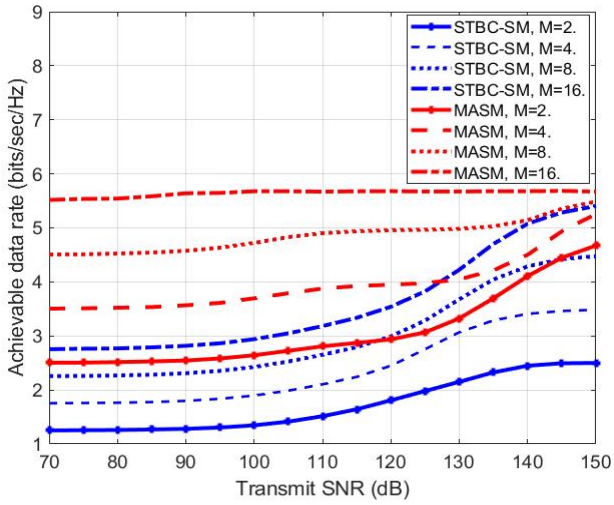


Fig. 6: The achievable rate performance comparison between STBC-SM and MASM versus transmit SNR. $N_t = 6$, $N_a = 2$, and $N_r = 1$.

for the the case of $N_t = 6, N_a = 3$, and $M = 2$, the percentage difference in the BER is almost 99.9999% compared to MASM. Additionally, it is noted that the BER performance of MASM is degraded as N_a increases which is attributed to the increased spatial interference between the active LEDs. Moreover, for fixed N_a and varying N_t, the BER performance for MASM drops noticeably because of the decreased separation and increased correlation between the LEDs. A similar remark can be also made for the case of increasing the modulation order M. On the contrary, STBC-SM is more robust to the change in the involved parameters in terms of the achievable BER. An interesting remark can be also concluded from the last two settings, i.e., $N_t = 7$ and $N_t = 8$. Specifically, even though we obtain the same spectral efficiency from the two configurations for the same values of N_a and M, it can be noticed that using lower N_t would results in a lower BER values. This is attributed to the increased separation, and hence, reduced interference between LEDs. However, in terms of throughput, it can be seen that MASM outperforms STBC-SM particularly for low modulation size. For instance, the percentage difference between the two schemes for $N_t = 6, N_a = 4$, and $M = 2$ is 68.9655%. Therefore, it is concluded that the BER related benefit of the proposed scheme is much greater compared to the throughput loss. Also, even though MASM outperforms STBC-SM in the achieved throughput, it is clear from the setting $N_t = 6, N_a = 2$, and $M = 16$ that the gap difference in the throughput decreases between both schemes for large modulation orders M. For instance, the percentage difference in terms of throughput for this case is 3.5088% relative to the MASM, which is very small compared to the case of $N_t = 6, N_a = 2$, and $M = 4$, where the percentage difference is 45.3125%. Therefore, this renders the proposed scheme more suitable for setups where the room has limited number of LEDs and high modulation order M. It is also noted here that using high-rate QOSTBC can assist towards reducing the throughput gap if it is integrated with SM.

It is well known that the performance of indoor VLC networks is very sensitive to the placement of the LEDs in the room. Hence, Fig.7 demonstrates the effect of varying the horizontal and the vertical separations between LEDs 1, 2, 3, and 4. It can be seen from the figure that there exists an optimum separation between the LEDs where both schemes achieve the best performance. This is explained as follows: the effect of the correlation is very high when the LEDs are very close to each other, which increases the error rate in the index detection. On the contrary, when the LEDs are placed considerably far from each other, the amount of the received power from each active LED is ultimately reduced. Therefore, an optimum placement of the LEDs which guarantees low correlation of the involved wireless channels and acceptable received amount of power is necessary. It is also noted that the proposed system is more robust to the LEDs' placement and achieves a good BER performance for various separation values.

Beside this, we present the effect of varying the half-power semi-angle ($\varphi_{1/2}$) of the LEDs on the BER performance for different values of transmit SNR, while fixing the other parameters. Fig. 8 shows the simulated and analytical BER versus the semi-angle for $N_t = 6$, $N_a = 2$, $M = 2$, and SNR values of 130 dB, 135 dB, and 140 dB. As expected, the MIMO system performance in VLC is highly dependent upon the value of $\varphi_{1/2}$ of the LEDs. As depicted in the figure, by fixing all other system parameters, the performance ultimately improves as the angle decreases due to the improved channel gains and the reduced correlation between different channels.

TABLE II: BER and throughput for different configurations

Involved Parameters			BER			Throughput		
N_t	N_a	M	STBC-SM	MASM	$\Delta\%$	$R_{stbc-sm}$	R_{sm}	$\Delta\%$
6	2	2	≈ 0	0.024	100	2.5	4.8	47.9167
6	3	2	2.4×10^{-9}	0.133	99.9999	2.3	6	61.6667
6	4	2	3.4×10^{-6}	0.171	99.9980	1.8	5.8	68.9655
6	2	2	≈ 0	0.024	100	2.5	4.8	47.9167
6	2	4	9.1×10^{-4}	0.084	98.9167	3.5	6.4	45.3125
6	2	16	0.005	0.475	98.9474	5.5	5.7	3.5088
4	2	2	≈ 0	8.9×10^{-5}	100	2	4	50
6	2	2	≈ 0	0.024	100	2.5	4.8	47.9167
7	2	2	7.5×10^{-9}	0.065	99.9999	3	5.6	46.4286
8	2	2	1.3×10^{-6}	0.079	99.9983	2.99	5.5	45.6363

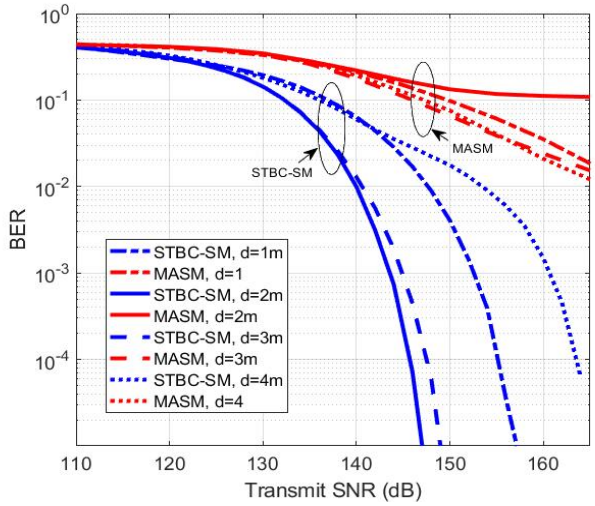


Fig. 7: Effect of varying the horizontal and the vertical separation d between LEDs 1, 2, 3, and 4. $N_t = 6$, $N_a = 2$, $N_r = 1$, and $M = 2$.

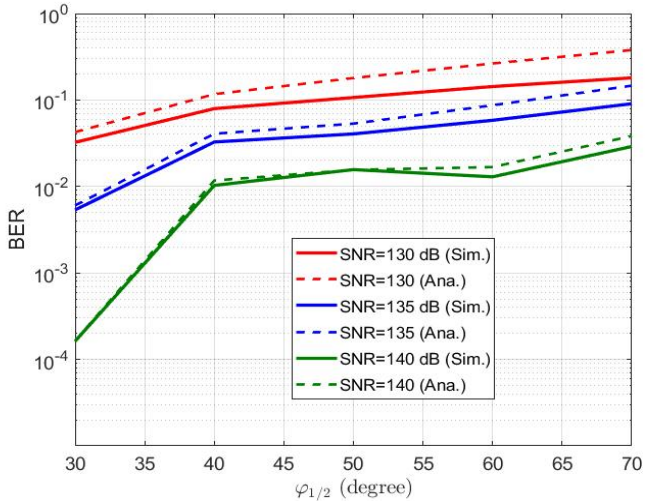


Fig. 8: Effect of varying $\varphi_{1/2}$ for different transmit SNR. $N_t = 6$, $N_a = 2$, $N_r = 1$, and $M = 2$.

Finally, we study the BER performance of the proposed high-rate QOSTBC-SM and compare its achievable performance with respect to MASM and RC-SM based schemes for different spectral efficiency values, i.e., η = 5 bpcu, 6 bpcu, and 7 bpcu. It can be seen from Fig. 9 that integrating QOSTBCs with SM enhances the system performance in terms of the achievable BER compared to MASM and RC-SM for fixed spectral efficiency values. This performance improvement can be noticed more profoundly at higher spectral efficiency values. For instance, a η = 7 bpcu spectral efficiency value was realized through QOSTBC-SM by choosing the system setup as follows: $N_t = 4, N_a = 2$, and $M = 8$, whereas the achieved error rate at SNR = 170 dB is 1.6×10^{-3}. On the contrary, in order to achieve the same spectral efficiency using RC-SM, the system setup was chosen as, $N_t = 4, N_a = 2$, and $M = 32$. However, the achieved error rate in this case considering the same SNR is 1.4×10^{-2}. The need for higher M-ary modulation values while fixing other system setup parameters explains the error rate performance gap between the two schemes at higher η values. However, at lower spectral efficiency values, i.e., 5 bpcu, RC-SM achieves better performance compared to both QOSTBC-SM and MASM. Besides this, since the proposed QOSTBC matrix has a rate of $R = 2$, it provides a spectral efficiency enhancement when integrated with SM compared to OSTBC-SM. Yet, this spectral efficiency enhancement comes at the expense of a slightly increased receiver complexity, which as already mentioned it is tolerable.

VI. Conclusion

In this paper, we considered the performance of a high-rate low complexity MIMO transmission STBC-SM scheme for VLC systems. A general technique has been proposed based on constructing any STBC-SM scheme for any M-ary PAM size and any number of transmitting LEDs. It has been shown through out simulations and derived upper bounds that STBC-SM is a promising MIMO technique for indoor VLC system

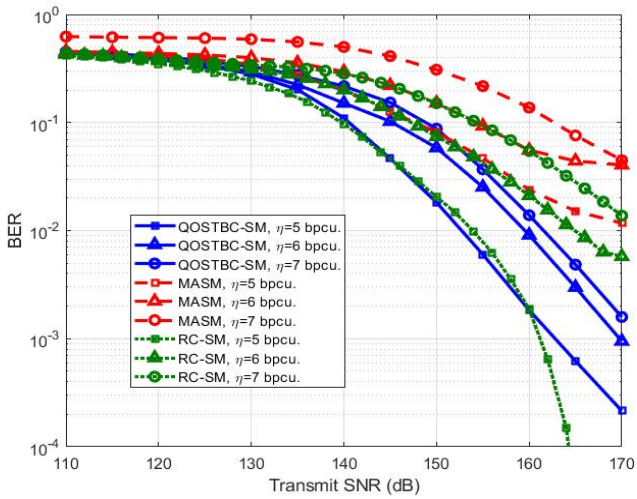


Fig. 9: BER performance comparison between the proposed QOSTBC-SM, MASM, and RC-SM. η = 5 bpcu, 6 bpcu, and 7 bpcu.

as it offers improved system BER performance, throughput and reduced receiver complexity compared to MASM and RC-SM. To achieve that, part of the bit stream was used to activate a group of the available LEDs, while the other part of the bit stream is conveyed through space time coded intensity modulation. Furthermore, it has been shown through extensive simulations that STBC-SM maintains a rather good performance for various setups, whilst an improved throughput is achieved compared to MASM as the modulation size increases.

REFERENCES

[1] E. Yaacoub and M. Alouini, "A key 6G challenge and opportunity—connecting the base of the pyramid: A survey on rural connectivity," *Proc. IEEE*, vol. 108, no. 4, pp. 533–582, Apr. 2020.

[2] O. I. Younus, H. Le Minh, P. T. Dat, N. Yamamoto, A. T. Pham, and Z. Ghassemlooy, "Dynamic physical-layer secured link in a mobile MIMO VLC system," *IEEE Photon. J.*, vol. 12, no. 3, pp. 1–14, June 2020.

[3] A. Jovicic, J. Li, and T. Richardson, "Visible Light Communication: Opportunities, Challenges and The Path To Market," *IEEE Commun. Mag.*, vol. 51, no. 12, pp. 26–32, Dec. 2013.

[4] T. Fath and H. Haas, "Performance comparison of MIMO techniques for optical wireless communications in indoor environments," *IEEE Trans. Commun.*, vol. 61, no. 2, pp. 733–742, Feb. 2013.

[5] H. S. Hussein and M. Hagag, "Optical MIMO-OFDM with fully generalized index-spatial LED modulation," *IEEE Commun. Lett.*, vol. 23, no. 9, pp. 1556–1559, Sept. 2019.

[6] S. S. Bawazir, P. C. Sofotasios, S. Muhaidat, Y. Al-Hammadi, and G. K. Karagiannidis, "Multiple access for visible light communications: Research challenges and future trends," *IEEE Access*, vol. 6, pp. 26 167–26 174, 2018.

[7] S. Singh and N. Sharma, "Error performance of burst-mode receivers," *IEEE Photon. J.*, vol. 2, no. 3, pp. 338–346, Jun. 2010.

[8] S. S. G. Surinder Singh, Hari Ram, "Performance evaluation of channel estimation in OFDM system for different QAM and PSK modulations," *International Journal of Electrical and Computer Engineering (IJECE)*, vol. 1, no. 2, pp. 140–150, Dec. 2011.

[9] P. M. Butala, H. Elgala, and T. D. C. Little, "Performance of optical spatial modulation and spatial multiplexing with imaging receiver," in *2014 IEEE Wireless Communications and Networking Conference (WCNC)*, April 2014, pp. 394–399.

[10] P. W. Wolniansky, G. J. Foschini, G. D. Golden, and R. A. Valenzuela, "V-BLAST: an architecture for realizing very high data rates over the rich-scattering wireless channel," in *1998 URSI International Symposium on Signals, Systems, and Electronics. Conference Proceedings (Cat. No.98EX167)*, Oct 1998, pp. 295–300.

[11] S. M. Khan, N. Saha, M. R. Rahman, M. Hasan, and M. S. Rahman, "Performance improvement of MIMO VLC using V-BLAST technique," in *2016 5th International Conference on Informatics, Electronics and Vision (ICIEV)*, May 2016, pp. 45–49.

[12] V. Tarokh, H. Jafarkhani, and A. R. Calderbank, "Space-time block codes from orthogonal designs," *" IEEE Trans. Inf. Theory*, vol. 45, no. 5, pp. 1456–1467, July 1999.

[13] J.-N. Guo, J. Zhang, Y.-Y. Zhang, G. Xin, and L. Li, "Constant weight space-time codes for dimmable MIMO-VLC systems," *IEEE Photon. J.*, vol. 12, no. 6, pp. 1–15, Dec. 2020.

[14] G. Ntogari, T. Kamalakis, and T. Sphicopoulos, "Performance analysis of space time block coding techniques for indoor optical wireless systems," *IEEE J. Sel. Areas Commun.*, vol. 27, no. 9, pp. 1545–1552, Dec. 2009.

[15] Y. Amano, K. Kamakura, and T. Yamazato, "Alamouti-type coding for visible light communication based on direct detection using image sensor," in *2013 IEEE Global Communications Conference (GLOBECOM)*, 2013, pp. 2430–2435.

[16] L. M. Hwang, Y. W. Kim, B. G. Choi, and K. S. Kim, "Performance of color shift keying-space time block code-orthogonal frequency division multiplexing system on visible light communication," in *The 2014 2nd International Conference on Systems and Informatics (ICSAI 2014)*, 2014, pp. 602–606.

[17] M. Biagi and A. M. Vegni, "Enabling high data rate vlc via mimo-leds ppm," in *2013 IEEE Globecom Workshops (GC Wkshps)*, 2013, pp. 1058–1063.

[18] M. Biagi, N. B. Hassan, K. Werfli, T.-C. Bui, and Z. Ghassemlooy, "Analysis and demonstration of quasi trace orthogonal space time block coding for visible light communications," *IEEE Access*, vol. 8, pp. 77 164–77 170, 2020.

[19] X. Cheng, M. Zhang, M. Wen, and L. Yang, "Index modulation for 5G: Striving to do more with less," *IEEE Wireless Commun.*, vol. 25, no. 2, pp. 126–132, Apr. 2018.

[20] T. Mao, Q. Wang, Z. Wang, and S. Chen, "Novel index modulation techniques: A survey," *Commun. Surveys Tuts.*, vol. 21, no. 1, pp. 315–348, Firstquarter 2019.

[21] M. Guo, Z. Bai, K. Pang, X. Hao, J. Tian, and K. Kwak, "Color space and multi-stream spatial modulation based indoor visible light communication," in *2020 International Wireless Communications and Mobile Computing (IWCMC)*, 2020, pp. 1091–1095.

[22] K. Cai and M. Jiang, "SM/SPPM aided multiuser precoded visible light communication systems," *IEEE Photon. J.*, vol. 8, no. 2, pp. 1–9, Apr. 2016.

[23] W. Popoola, E. Poves, and H. Haas, "Generalised space shift keying for visible light communications," in *2012 8th International Symposium on Communication Systems, Networks Digital Signal Processing (CSNDSP)*, July 2012, pp. 1–4.

[24] Q. Zhang, Z. Bai, N. Zhang, S. Sun, and K. S. Kwak, "Performance analysis of DC-SSK scheme and its power allocation in VLC system," in *2018 International Conference on Computing, Networking and Communications (ICNC)*, 2018, pp. 280–284.

[25] F. Wang, C. Liu, Q. Wang, J. Zhang, R. Zhang, L. Yang, and L. Hanzo, "Secrecy analysis of generalized space-shift keying aided visible light communication," *IEEE Access*, vol. 6, pp. 18 310–18 324, 2018.

[26] N. Su, E. Panayirci, M. Koca, A. Yesilkaya, H. Vincent Poor, and H. Haas, "Physical layer security for multi-user MIMO visible light communication systems with generalized space shift keying," *IEEE Trans. Commun.*, vol. 69, no. 4, pp. 2585 – 2598, Apr. 2021.

[27] R. Mesleh, H. Haas, C. W. Ahn, and S. Yun, "Spatial modulation - a new low complexity spectral efficiency enhancing technique," in *2006 First International Conference on Communications and Networking in China*, Oct 2006, pp. 1–5.

[28] J. Wang, H. Ge, M. Lin, J. Wang, J. Dai, and M. Alouini, "On the secrecy rate of spatial modulation-based indoor visible light communications," *IEEE J. Sel. Areas Commun.*, vol. 37, no. 9, pp. 2087–2101, Sept. 2019.

[29] M. Le Tran and S. Kim, "Receiver-oriented spatial modulation in visible light communication system," *IEEE Access*, vol. 7, pp. 129 666–129 677, 2019.

[30] X. Gao, Z. Bai, P. Gong, and D. O. Wu, "Design and performance analysis of LED-grouping based spatial modulation in the visible light communication system," *IEEE Trans. Veh. Technol.*, vol. 69, no. 7, pp. 7317–7324, July 2020.

[31] Z. Zheng, H. Du, J. Xue, and Z. Wu, "Adaptive spatial modulation for indoor visible light communications," *IEEE Commun. Lett.*, vol. 24, no. 10, pp. 2240–2244, Oct. 2020.

[32] J. Wang, H. Ge, J. Zhu, J. Wang, J. Dai, and M. Lin, "Adaptive spatial modulation for visible light communications with an arbitrary number of transmitters," *IEEE Access*, vol. 6, pp. 37 108–37 123, 2018.

[33] J. Wang, J. Zhu, S. Lin, and J. Wang, "Adaptive spatial modulation based visible light communications: SER analysis and optimization," *IEEE Photon. J.*, vol. 10, no. 3, pp. 1–14, Jun. 2018.

[34] C. Chen, Y. Yang, X. Deng, P. Du, H. Yang, Z. Chen, and W. Zhong, "NOMA for MIMO visible light communications: A spatial domain perspective," in *2019 IEEE Global Communications Conference (GLOBECOM)*, 2019, pp. 1–6.

[35] A. M. Aljaberi, S. A. Naser, P. C. Sofotasios, and S. Muhaidat, "Space shift keying modulation in non-orthogonal multiple access hybrid visible light communication systems (invited paper)," in *2020 3rd International Conference on Advanced Communication Technologies and Networking (CommNet)*, 2020, pp. 1–5.

[36] T. Wu, Z. Wang, J. Yu, and S. Han, "Performance analysis of NOMA VLC system using SM," in *2020 IEEE 5th Optoelectronics Global Conference (OGC)*, 2020, pp. 48–51.

[37] L. Qiu and M. Jiang, "A generalized spatial modulation for indoor optical wireless communications," in *2015 Opto-Electronics and Communications Conference (OECC)*, 2015, pp. 1–3.

[38] C. Rajesh Kumar and R. K. Jeyachitra, "Power efficient generalized spatial modulation MIMO for indoor visible light communications," *IEEE Photon. J.*, vol. 29, no. 11, pp. 921–924, Jun. 2017.

[39] D. Li, W. Zhang, J. Sun, and C. Wang, "An improved generalized spatial modulation scheme for indoor visible light communications," in *2017 IEEE/CIC International Conference on Communications in China (ICCC)*, Oct 2017, pp. 1–5.

[40] T. Datta, H. S. Eshwaraiah, and A. Chockalingam, "Generalized space-and-frequency index modulation," *IEEE Trans. Veh. Technol.*, vol. 65, no. 7, pp. 4911–4924, July 2016.

[41] M. Al-Nahhal, E. Basar, and M. Uysal, "Flexible generalized spatial modulation for visible light communications," *IEEE Trans. Veh. Technol.*, vol. 70, no. 1, pp. 1041–1045, Jan. 2021.

[42] M. Le Tran and S. Kim, "Novel bit mapping for generalized spatial modulation in VLC systems," *IEEE Photon. Technol. Lett.*, vol. 31, no. 15, pp. 1257–1260, Aug. 2019.

[43] Y. Xiao and Y. Zhu, "Chromaticity-adaptive generalized spatial modulation for MIMO VLC with multi-color LEDs," *IEEE Photon. J.*, vol. 11, no. 4, pp. 1–12, Aug. 2019.

[44] C. R. Kumar and R. K. Jeyachitra, "Improved joint generalized spatial modulations for MIMO-VLC systems," *IEEE Commun. Lett.*, vol. 22, no. 11, pp. 2226–2229, Nov. 2018.

[45] E. Curry and D. K. Borah, "Iterative combinatorial symbol design for spatial modulations in MIMO VLC systems," *IEEE Photon. Technol. Lett.*, vol. 30, no. 5, pp. 483–486, March 2018.

[46] M. K. Jha, N. Kumar, and Y. V. S. Lakshmi, "Flip-OFDM based generalized spatial MIMO for VLC," in *2019 PhD Colloquium on Ethically Driven Innovation and Technology for Society (PhD EDITS)*, 2019, pp. 1–2.

[47] H. S. Hussein and M. Hagag, "Optical MIMO-OFDM with fully generalized index-spatial LED modulation," *IEEE Commun. Lett.*, vol. 23, no. 9, pp. 1556–1559, 2019.

[48] Xiang-chuan Gao, Jian-kang Zhang, and J. Jin, "Linear space codes for indoor MIMO visible light communications with ML detection," in *2015 10th International Conference on Communications and Networking in China (ChinaCom)*, Aug 2015, pp. 142–147.

[49] M. Biagi, A. M. Vegni, S. Pergoloni, P. M. Butala, and T. D. C. Little, "Trace-orthogonal PPM-space time block coding under rate constraints for visible light communication," *J. Lightw. Technol.*, vol. 33, no. 2, pp. 481–494, Jan. 2015.

[50] Z. Ghassemlooy, W. Popoola, and S. Rajbhandari, *Optical Wireless Communications: System and Channel Modelling with MATLAB®, Second Edition*. CRC Press, 05 2019.

[51] T. Komine and M. Nakagawa, "Fundamental Analysis for Visible-Light Communication System Using LED Lights," *IEEE Trans. Consum. Electron.*, vol. 50, no. 1, pp. 100–107, Feb. 2004.

[52] L. Bariah, S. Muhaidat, and A. Al-Dweik, "Error probability analysis of non-orthogonal multiple access over nakagami- m fading channels," *IEEE Trans. Commun.*, vol. 67, no. 2, pp. 1586–1599, Feb. 2019.

[53] T. Fath and H. Haas, "Optical spatial modulation using colour leds," in *2013 IEEE International Conference on Communications (ICC)*, 2013, pp. 3938–3942.

[54] C. He, T. Q. ang, and J. Armstrong, "Performance of optical receivers using photodetectors with different fields of view in a MIMO ACO-OFDM system," *J. Lightw. Technol.*, vol. 33, no. 23, pp. 4957–4967, Dec. 2015.

[55] L. Yin, W. O. Popoola, X. Wu, and H. Haas, "Performance evaluation of non-orthogonal multiple access in visible light communication," *IEEE Trans. Commun.*, vol. 64, no. 12, pp. 5162–5175, Dec. 2016.

[56] A. Stavridis and H. Haas, "Performance evaluation of space modulation techniques in vlc systems," in *2015 IEEE International Conference on Communication Workshop (ICCW)*, 2015, pp. 1356–1361.



Shimaa Naser received the M.Sc. degree in Electrical Engineering from the University of Science and Technology, Irbid, Jordan in 2015. Since 2018, she is pursuing her Ph.D. degree at the Department of Electrical and Computer Engineering at Khalifa University, Abu Dhabi, UAE. Her research interests include advanced digital signal processing and modulation techniques for visible light communications, MIMO-based communiaction, and orthogonal/non-orthogonal multiple access.



Lina Bariah (S'13-M'19) received the M.Sc. and Ph.D degrees in communications engineering from Khalifa University, Abu Dhabi, United Arab Emirates, in 2015 and 2018. She is currently a Post-doctoral fellow with the KU Center for Cyber-Physical Systems, Khalifa University, UAE. She was a Visiting Researcher with the Department of Systems and Computer Engineering, Carleton University, ON, Canada, in summer 2019. Her research interests include advanced digital signal processing techniques for communications, channel estimation, cooperative communications, non-orthogonal multiple access, cognitive radios, and intelligent surfaces.



Sami Muhaidat (S'01-M'08-SM'11) received the Ph.D. degree in electrical and computer engineering from the University of Waterloo, Waterloo, ON, Canada, in 2006. From 2007 to 2008, he was an NSERC Post-Doctoral Fellow with the Department of Electrical and Computer Engineering, University of Toronto, ON, Canada. From 2008 to 2012, he was Assistant Professor with the School of Engineering Science, Simon Fraser University, Burnaby, BC, Canada. He is currently an Associate Professor with Khalifa University, Abu Dhabi, UAE, and a Visiting Professor with the Department of Electrical and Computer Engineering, University of Western Ontario, London, ON, Canada. He is also a Visiting Reader with the Faculty of Engineering, University of Surrey, Guildford, U.K. Dr. Muhaidat currently serves as an Area Editor of the IEEE TRANSACTIONS ON COMMUNICATIONS, and he was previously a Senior Editor of the IEEE COMMUNICATIONS LETTERS and an Associate Editor of IEEE TRANSACTIONS ON COMMUNICATIONS, IEEE COMMUNICATIONS LETTERS and IEEE TRANSACTIONS ON VEHICULAR TECHNOLOGY. He was a recipient of several scholarships during his undergraduate and graduate studies and the winner of the 2006 NSERC PostDoctoral Fellowship Competition. Dr Muhaidat is a Senior Member IEEE.



Mahmoud Al-Qutayri (S'87, M'92, SM'02) is the Associate Dean for Graduate Studies – College of Engineering, and a Professor of Electrical and Computer Engineering at Khalifa University, UAE. He received the B.Eng., MSc and PhD degrees from Concordia University, Canada, University of Manchester, U.K., and the University of Bath, U.K., all in Electrical and Electronic Engineering in 1984, 1987, and 1992, respectively. Prior to joining Khalifa University, he was a Senior Lecturer at De Montfort University, UK. This was preceded by a Research Officer appointment at University of Bath, UK. He has published numerous technical papers in peer reviewed international journals and conferences. He coauthored a book as well as a number of book chapters. His main fields of research include embedded systems design, applications and security, design and test of mixed-signal integrated circuits, wireless sensor networks, and cognitive wireless networks. During his academic career, Dr. Al-Qutayri made many significant contributions to both undergraduate as well as graduate education. His professional service includes membership of the steering, organizing and technical program committees of many international conferences.



Murat Uysal (Fellow, IEEE) received the B.Sc. and the M.Sc. degree in electronics and communication engineering from Istanbul Technical University, Istanbul, Turkey, in 1995 and 1998, respectively, and the Ph.D. degree in electrical engineering from Texas A&M University, College Station, Texas, in 2001. He is currently a Full Professor and Chair of the Department of Electrical and Electronics Engineering at Özyeğin University, Istanbul, Turkey. He also serves as the Founding Director of Center of Excellence in Optical Wireless Communication Technologies (OKATEM). Prior to joining Özyeğin University, he was a tenured Associate Professor at the University of Waterloo, Canada. Dr. Uysal's research interests are in the broad area of communication theory with a particular emphasis on the physical layer aspects of wireless communication systems in radio and optical frequency bands. On these topics, he has authored some 350 journal and conference papers and received more than 14.000 citations with an h-index of 56. Prof. Uysal is an IEEE Fellow and the former Chair of IEEE Turkey Section. He currently serves on the editorial board of IEEE Transactions on Wireless Communications. In the past, he served as an Editor for IEEE Transactions on Communications, IEEE Transactions on Vehicular Technology, and IEEE Communications Letters. He was involved in the organization of several IEEE conferences at various levels. In particular, he served as the Technical Program Committee Chair of major IEEE conferences including WCNC 2014, PIMRC 2019 and VTC-Fall 2019. Prof Uysal's major distinctions include NSERC Discovery Accelerator Award in 2008, University of Waterloo Engineering Research Excellence Award in 2010, Turkish Academy of Sciences Distinguished Young Scientist Award in 2011, Özyeğin University Best Researcher Award in 2014, National Instruments Engineering Impact Award in 2017, Elginkan Foundation Technology Award in 2018 and IEEE Communications Society Best Survey Paper Award in 2019 among others.



Paschalis C. Sofotasios (S'07-M'12-SM'16) was born in Volos, Greece, in 1978. He received the M.Eng. degree from Newcastle University, U.K., in 2004, the M.Sc. degree from the University of Surrey, U.K., in 2006, and the Ph.D. degree from the University of Leeds, U.K., in 2011. He has held academic positions at the University of Leeds, U.K., University of California at Los Angeles, CA, USA, Tampere University of Technology, Finland, Aristotle University of Thessaloniki, Greece and Khalifa University of Science and Technology, UAE, where he currently serves as Assistant Professor in the department of Electrical Engineering and Computer Science. His M.Sc. studies were funded by a scholarship from UK-EPSRC and his Doctoral studies were sponsored by UK-EPSRC and Pace plc. His research interests are in the broad areas of digital and optical wireless communications as well as in topics relating to special functions and statistics. Dr. Sofotasios serves as a regular reviewer for several international journals and has been a member of the technical program committee of numerous IEEE conferences. He currently serves as an Editor for the IEEE COMMUNICATIONS LETTERS and he received the Exemplary Reviewer Award from the IEEE COMMUNICATIONS LETTERS in 2012 and the IEEE TRANSACTIONS ON COMMUNICATIONS in 2015 and 2016. Dr. Sofotasios is a Senior Member IEEE and he received the Best Paper Award at ICUFN 2013.